International Journal of Fatigue 43 (2012) 150–159

Contents lists available at SciVerse ScienceDirect

International Journal of Fatigue

journal homepage: www.elsevier.com/locate/ijfatigue

Enabling high-order integration of fatigue crack growth with surrogate modeling

Matthew J. Pais, Felipe A.C. Viana, Nam H. Kim *

Department of Mechanical and Aerospace Engineering, College of Engineering, University of Florida, PO Box 116250, Gainesville, FL 32611, United States

ARTICLE INFO

Article history:
Received 4 March 2011
Received in revised form 19 March 2012
Accepted 22 March 2012
Available online 29 March 2012

Keywords:
Fatigue
Crack growth
Fracture mechanics
Surrogate model
Extended finite element method

ABSTRACT

Modeling fatigue crack growth is computationally challenging because the crack growth rate can only be evaluated at the current crack size. Therefore, the forward Euler method has been a common choice in integrating fatigue crack growth. However, since its accuracy can only be guaranteed with a small step size, the method cannot be applied to the investigation of systems with complex geometry (calling for expensive finite element simulations). Higher-order integration methods, such as the midpoint method, allow larger step size but require evaluation of crack growth rate at crack sizes larger than the current one. In arbitrary geometry, this is not an easy task because the direction of crack growth is unknown in advance. In this paper, surrogate models are generated for the prior crack growth direction and stress intensity factor data. These surrogates are cheap to evaluate and predict the crack growth rate without the need of additional finite element simulations. The step size for the numerical integration is chosen based on the accuracy of the extrapolated crack growth predictions for direction and stress intensity factor. Several examples were tested in which crack growth follows linear and curved paths under a range of boundary conditions leading to different relationships between stress intensity factor and crack size. Results showed that a large increase in the allowable step size may be used with increased accuracy over the Euler method with the need for fewer expensive function evaluations.

1. Introduction

Modeling fatigue crack growth is a challenging problem in computational fracture mechanics. Fatigue crack growth is commonly governed by an ordinary differential equation of the general form [1]

$$\frac{da}{dN} = f(\Delta K, R) \tag{1.1}$$

where ΔK is the stress intensity factor range and R is the stress ratio. The relationship given in Eq. (1.1) is typically a monotonically increasing function as shown in Fig. 1 (the exact curves depend on geometry, loading conditions, and material properties).

Integration of Eq. (1.1) is expensive because evaluation of $f(\Delta K, R)$ usually requires high-fidelity physics-based modeling (such as those obtained with the finite element method[1] [2,5,6]). It is also computationally intensive because the large number of loading cycles (10^3–10^8) for failure requires a large number of simulations. As a result, the applications might be limited to relatively simple geometries (because ΔK depends on the characteristic crack length a, except for very simple cases [7,8]). Sankararaman et al. [9] used a Gaussian process surrogate to replace expensive finite element simulations when predicting fatigue crack growth.

The two traditional approaches to numerically integrate the crack growth are (a) to assume a fixed increment of crack growth for each crack geometry or (b) to assume a constant number of cycles elapses between each crack geometry [3,4,6]. The former uses an initially large number of elapsed cycles for a given crack geometry because the rate of crack growth is slow, and gradually decreases the number of cycles as the rate increases. Evaluating fatigue crack growth directly in terms of the number of elapsed cycles is challenging because the crack grows rapidly as it approaches the critical crack size, leading to numerical instability [5,6].

Forward Euler approximation [10] has been used to solve the fatigue crack growth model [11]. The main advantage is that $f(\Delta K, R)$ is evaluated only at the current crack geometry. Unfortunately, there are two major drawbacks associated with the forward Euler method. First, it requires a small step size to maintain stability and accuracy of the solution. Second, due to the monotonic behavior of $f(\Delta K, R)$ (see Fig. 1), the method will always under predict a and ΔK from N and over predict ΔK from a, increasing the error as integration progresses. Higher-order

* Corresponding author. Tel.: +1 352 575 0665; fax: +1 352 392 7303.
E-mail addresses: mpais@ufl.edu (M.J. Pais), fchegury@ufl.edu (F.A.C. Viana), nkim@ufl.edu (N.H. Kim).

[1] When using classical finite element approaches, there are also challenges associated with meshing the crack tip. Remeshing [2] as growth occurs is a difficult task and can be avoided through the use of the extended finite element method [3,4] (XFEM). Through a series of XFEM simulations, it is possible to generate data points and approximate the right-hand side of Eq. (1.1). Until the completion of the finite element simulations, $f(\Delta K, R)$ is an unknown function.

0142-1123/$ - see front matter © 2012 Elsevier Ltd. All rights reserved.
http://dx.doi.org/10.1016/j.ijfatigue.2012.03.010

Nomenclature

a_k	target percent error in kriging surrogate for ΔK
a_t	target percent error in kriging surrogate for θ
a_N	crack length at cycle N
K_I	Mode I stress intensity factor
K_{II}	Mode II stress intensity factor
N_i	cycle corresponding to current crack geometry
$N_{i+1/2}$	cycle corresponding to midpoint between current and next crack geometry
N_{i+1}	cycle corresponding to next crack geometry
α_k	rate of change in ΔN_{i+1} due to a_k
α_t	rate of change in ΔN_{i+1} due to a_t
Δa	crack growth increment
ΔK	stress intensity factor range
ΔK_i	stress intensity factor range at cycle N_i
$\Delta K_{i+1/2}$	stress intensity factor range at cycle $N_{i+1/2}$
ΔK_{i+1}	stress intensity factor range at cycle N_{i+1}
ΔK_{i+1}^{NUM}	stress intensity factor range at cycle N_{i+1} from numerical method
ΔK_{i+1}^{SUR}	stress intensity factor range at cycle N_{i+1} from surrogate model
ΔK_{eq}	equivalent stress intensity factor range
ΔK_I	Mode I stress intensity factor range
ΔK_{II}	Mode II stress intensity factor range
ΔN	number of elapsed cycles
ΔN_i	number of elapsed cycles between cycles N_i and N_{i+1}
ΔN_{i+1}	number of elapsed cycles between cycles N_{i+1} and N_{i+2}
θ	crack growth direction in crack tip coordinate system
θ_{i+1}^{NUM}	stress intensity factor range at cycle N_{i+1} from numerical method
θ_{i+1}^{SUR}	stress intensity factor range at cycle N_{i+1} from surrogate model

approximations such as the midpoint method could be used to address this issue, but such methods require additional function evaluations needed for slope computation (besides increased computational cost such computations cannot be done at the present integration step. After all, the crack geometry is known only up to that point).

This paper, propose the use of surrogate models to enable such higher-order integrators. Surrogate modeling (also known as metamodeling or response surface approximation) consists of analyzing a number of designs, fitting a surrogate, then replacing the costly simulations by the surrogate model [12–15]. The basic idea is to use the history of stress intensity factors as a function of either number of cycles or crack lengths up to the current cycle to build a surrogate model and predict the stress intensity factor at different crack sizes or different cycles. New data points can be added to the original set as the simulation evolves and more data points are available for the surrogate model.

Here three cases are considered. First, for a fixed increment of crack growth Δa (or a fixed number of elapsed cycles ΔN), the relationship between ΔK and Δa is fitted using a kriging surrogate. Second, a variable step size algorithm is introduced for the automatic generation of a step size Δa (or ΔN) based on the accuracy in the surrogate extrapolation of ΔK and the crack growth direction. This is an attempt to only perform expensive function evaluations when needed. Third, the case of mixed-mode crack growth is considered and the use of a surrogate model enables approximation to the crack growth direction.

Two examples with known relationships between ΔK and a are used to illustrate how the proposed methodology enable accurate high order integration: a center crack in an infinite plate under uniaxial tension and an edge crack in a finite plate. In another example, the extended finite element method is used to model mixed-mode crack growth for an inclined center crack in a finite plate and an edge crack in a finite plate with a hole. The results show that kriging enables large step sizes without sacrificing accuracy.

The remainder of the paper is organized as follows. In Section 2 the crack growth model is introduced which consists of the fatigue crack growth model, traditional solution procedures, equivalent stress intensity factor range for mixed-mode loading, and crack growth direction. In Section 3 the use of a surrogate model for higher-order integration is introduced along with a variable step size algorithm based upon the agreement between the surrogate predictions and function evaluations. In Section 4 three numerical experiments are conducted to test the proposed algorithms for a several crack geometries, initial crack sizes, and materials. Finally, in Section 5 conclusions are drawn about enabling higher-order integration through surrogate models.

2. Crack growth model

2.1. Fatigue crack growth model

One of the first attempts to create a model to represent fatigue crack growth was that of Paris [16]. Many modified versions of the Paris model attempt to address areas which the Paris model neglects such as crack closure [1,17,18], stress ratio R [19–21], and the threshold stress intensity factor [1,21–23]. Other models include the state-space model [24,25] and the small time scale model [26] which have an emphasis on modeling variable amplitude

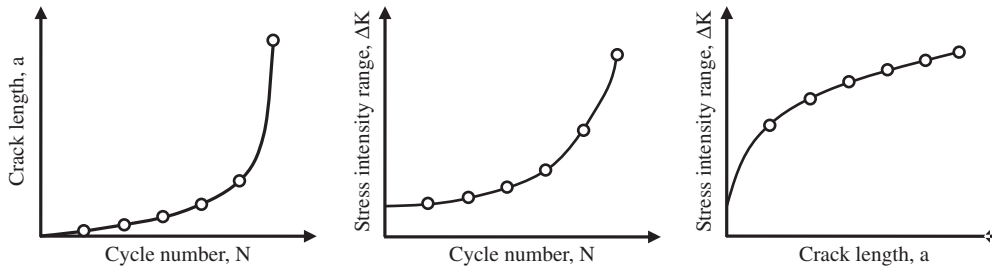

Fig. 1. The relationships between stress intensity factor range ΔK, crack length a, and number of cycles N. While the true curves are continuous as denoted by the solid lines, they are commonly discretized into a finite number of points as shown by the open circles in each figure in order to reduce the number of function evaluations needed to approximate the system.

loading. For simplicity, the Paris model is used within this paper, but the principles could be applied to any crack growth model governed by an ordinary differential equation. The Paris model is given as

$$\frac{da}{dN} = C(\Delta K)^m \tag{2.1}$$

where da/dN is the crack growth rate, C and m are model parameters, and ΔK is the range of Mode I stress intensity factor. An analytical solution of Eq. (2.1) is available for the simplest case that is an infinite plate under Mode I loading. Other cases require numerical integration in order to calculate the crack growth as a function of fatigue loading cycle N.

The solution of Eq. (2.1) with respect to modeling crack growth with finite element simulations has taken two main approaches. First, a fixed crack growth increment Δa can be considered. Once the simulations have completed, the relation between Δa and ΔK can be used to find the corresponding ΔN for each function evaluation. For a fixed increment of elapsed cycles ΔN can be considered. Here, for a given crack geometry Δa is approximated based on the selected ΔN and the current function evaluation's prediction of ΔK. Either method is capable of yielding an accurate representation of the fatigue crack growth behavior for a given structure, should an appropriate step size of Δa or ΔN be chosen. Second, an automated variable step size algorithm has been introduced to distribute the simulations in a controlled manner with the goal of reducing the number of simulations needed without a loss in accuracy.

When there are nonzero Mode II stress intensity factors present, it is necessary to consider an equivalent stress intensity factor range as well as a direction of crack growth. There are many ways to find an equivalent stress intensity factor range [23,27–29]. Here the method proposed by Tanaka [28] is used:

$$\Delta K_{eq} = \sqrt[4]{\Delta K_I^4 + 8\Delta K_{II}^4} \tag{2.2}$$

where ΔK_I and ΔK_{II} are the ranges of Modes I and II stress intensity factors, respectively.

The direction of crack growth can be found from many methods [3,4,23,30–34], but here is assumed to be the direction which will maximize the opening Mode I stress intensity factor. This angle for any combination of mixed mode loading consisting of Modes I and II is given by the maximum circumferential stress criterion [3] as

$$\theta = 2\arctan\frac{1}{4}\left(\frac{K_I}{K_{II}} - sign(K_{II})\sqrt{\left(\frac{K_I}{K_{II}}\right)^2 + 8}\right). \tag{2.3}$$

Note, that this is in essence an Euler approximation to the crack growth direction as it only considers the stress intensity factors at the ith data point. As mentioned before, when the geometry of the plate is finite and the applied load generates mixed mode, it is not easy to calculate $\Delta K_{i+1/2}$. This requires building a finite element model with the crack geometry at $i + 1/2$. However, without knowing the crack geometry at $i + 1/2$, it is not possible to evaluate $\Delta K_{i+1/2}$. Thus, except for the forward Euler method, some kind of approximation should be adopted to estimate the range of stress intensity factors at the advanced location. In the following section, a surrogate modeling technique will be presented to approximate the range of stress intensity factor as well as the crack growth direction allowing for a midpoint approximation to be applied to both the magnitude and direction of crack growth for a given crack through the use of surrogate modeling.

2.2. Numerical integration of the fatigue crack growth model

2.2.1. Forward Euler method

For an arbitrary differential equation of the form $y'(x) = f(x, y(x))$ the goal is to predict the value of y_{n+1} while the current data is available up to y_n. The simplest numerical method available which is applicable to the current crack growth problem is the explicit forward Euler method [10] given as

$$y_{n+1} = y_n + hf(x_n, y_n) \tag{2.4}$$

where h is the step size from x_n to x_{n+1}. Note that $f(x_n, y_n)$ is the slope of $y(x)$ at x_n; therefore a linear approximation is being made from x_n to x_{n+1} using the slope at the x_n. This method has been popular in engineering applications because it only requires evaluating the slope at the current step, which often required expensive computational simulation. For example, in the case of crack growth simulation, $f(x_n, y_n)$ corresponds to calculating the stress intensity factor with given crack size y_n. Therefore, evaluating $f(x_n, y_n)$ requires a finite element modeling with the current geometry of the crack. If a different method, such as the backward Euler method, is used, then $f(x_{n+1}, y_{n+1})$ is required, which is the stress intensity factor corresponding to the unknown crack size y_{n+1}. Therefore, there exists a fundamental difficulty to use a numerical integration method other than the forward Euler method.

The simplest approach to integrate the Paris model for fatigue crack growth is the use of the forward Euler method. Here the stress intensity factor range at the current crack geometry is the only information needed to find the increment of growth between the current and future crack geometries. The growth increment is calculated as

$$\Delta a_i = \Delta N[C(\Delta K_i)^m] \tag{2.5}$$

where i is the current increment. The corresponding number of elapsed cycles can be approximated as

$$\Delta N_i = \frac{\Delta a}{C(\Delta K_i)^m} \tag{2.6}$$

for a fixed increment of crack growth. As the forward Euler method only uses the slope at the current point and linearly interpolates to the next crack size it can lead to large inaccuracies for relatively small crack growth increments. Although the physical meaning of ΔN is the number of elapsed cycles, in this model it is treated as a continuous variable as crack growth occurs over tens of thousands of cycles. Choosing a larger ΔN results in needing fewer finite element simulations while sacrificing accuracy.

Although the forward Euler method can resolve the issue related to evaluating the slope at unknown crack sizes, it has a drawback in slow convergence; the accuracy of the method is proportional to the step size, h. In crack growth analysis, the step size, ΔN, is the number of fatigue loading cycles between two evaluation points. Since cracks grow slowly throughout the lifecycle of a product, a small step size means tens of thousands of simulations. Therefore, it is highly desired to use a numerical integration method that allows a larger step size, while maintaining accuracy.

2.2.2. Midpoint integration method

There are numerous numerical methods that allow larger step sizes for integration, but the midpoint integration method is used as a demonstration tool in this paper. The midpoint method [10] generally provides a better accuracy than the forward Euler method as it takes the slope at the midpoint between the current and future data points $x_{n+1/2}$ and uses that value to approximate the interval from x_n to x_{n+1} such that the approximation is given as

$$y_{n+1} = y_n + hf\left(x_n + \frac{h}{2}, y_n + \frac{h}{2}f(x_n, y_n)\right). \tag{2.7}$$

The accuracy of the method is proportional to h^2; therefore, it allows a larger step size for the same accuracy with the forward Euler method. However, this method requires evaluating the slope at the advanced half step. In practice, this is not an easy task because the crack size at the advanced step is unknown; it is a part of the solution. In addition, in a complex system, the direction of crack growth may not be constant, and thus, it would be difficult to build a numerical model to calculate the slope at the advanced step.

The next approach to integrating the Paris model is the use of the midpoint method where the growth increment is calculated as

$$\Delta a_i = \Delta N[C(\Delta K_{i+1/2})^m] \tag{2.8}$$

where $i + 1/2$ is the midpoint between the current and next increment. Similarly, ΔN_i is given as

$$\Delta N_i = \frac{\Delta a}{C(\Delta K_{i+1/2})^m}. \tag{2.9}$$

Here the slope at the midpoint of the current cycle is use to extrapolate ahead to $i + 1$. This leads to a better approximation of the crack size at the next increment as a more accurate approximation of the slope over the entire interval of the chosen growth increment is used. This method requires additional function evaluations at $i + 1/2$ for each crack geometry, effectively doubling the number of function evaluations needed for the given simulation.

3. Use of surrogate model in integration

3.1. Constant step size algorithm

The limitation on the types of methods which can be used in the direct integration of a fatigue model come from the need to evaluate the stress intensity factor at some future crack tip position. Because this crack position is unknown, it is unclear how to apply a numerical method to address this challenge. The idea presented here is to use a surrogate model to fit the available stress intensity factor history. The surrogate model can then be used to extrapolate ahead of the current crack position to get an estimate of the stress intensity factor which can then be used for a higher-order integration method. Visually, this is shown in Fig. 2 where the filled circles represent current or past numerical data points, the empty circle represents the data point being solved for currently, and the empty square represents the function evaluation at the $N_{i+1/2}$.

In this paper, results are presented for the kriging surrogate (see Appendix A for details). Kriging was chosen after quick benchmark tests comparing other surrogates such as polynomial response surfaces [35], radial basis neural networks [36], and support vector regression [37]. Nevertheless, the techniques are suitable for any surrogate and the choice of which is problem dependent. A comprehensive study comparing surrogate performance is an objective of future research.

For problems with mixed mode loading, two kriging surrogates are used. First, a kriging surrogate is used to approximate the response of ΔK as a function of either the crack length a or the number of elapsed cycles N. The kriging approximation is then used for a higher order approximation to Paris moldel, such as the midpoint method given by Eq. (2.8). For the case of a fixed Δa, ΔN is calculated *a posteriori* to the function evaluations using interpolation between data points. Equally spaced data points between a_i and the final crack length are fitted using kriging. This surrogate is then used to interpolate between data points and evaluate the corresponding ΔN for each Δa. For a fixed ΔN, kriging is used to fit the data up to the current cycle and extrapolate approximate values of ΔK for the use of the midpoint method. Second, a kriging surrogate is used to approximate the angle of crack growth θ.

In order to build the surrogate model, at least three data points are required, which are obtained using the forward Euler method with a small time step. In addition, the initial crack grows slowly, i.e., small Δa, the forward Euler method can yield accurate crack growth calculation. Two algorithms are provided for the selection of a variable step size for direct fatigue evaluation. A general form is introduced based on the agreement between the stress intensity factor and crack growth direction values for the surrogate extrapolation and the theoretical or XFEM values.

3.2. Variable step size

There are numerical methods which will automatically adjust the integration step size to some allowable error [10]. However, these methods typically use function evaluations to estimate the error associated with a given step size before choosing upon a step size to use. In the finite element framework, this algorithm would result in expensive function evaluations in order to determine the allowable step size. To avoid these additional function evaluations, an algorithm is proposed which allows for the step size to be dynamically changed based on the accuracy of the surrogate extrapolation. The step size at the ith step is adjusted at $i + 1$th step according to the surrogate accuracy. That is, the more accurate the surrogate is, the larger the $i + 1$th step size will be. Conversely, if the surrogate is not accurate enough, the step size is reduced. Formally, the $i + 1$th step size is found from the solution for the ith crack geometry as

$$\Delta N_{i+1} = \Delta N_i \min\left[\left(\frac{a_k}{1-\frac{\Delta K_{i+1}^{SUR}}{\Delta K_{i+1}^{NUM}}}\right)^{\alpha_k}, \left(\frac{a_t}{\left|1-\frac{\theta_{i+1}^{SUR}}{\theta_{i+1}^{NUM}}\right|}\right)^{\alpha_t}\right] \tag{3.1}$$

where ΔN_i is the current step size, a is the allowable percent difference between the surrogate extrapolation and XFEM values at $i + 1$,

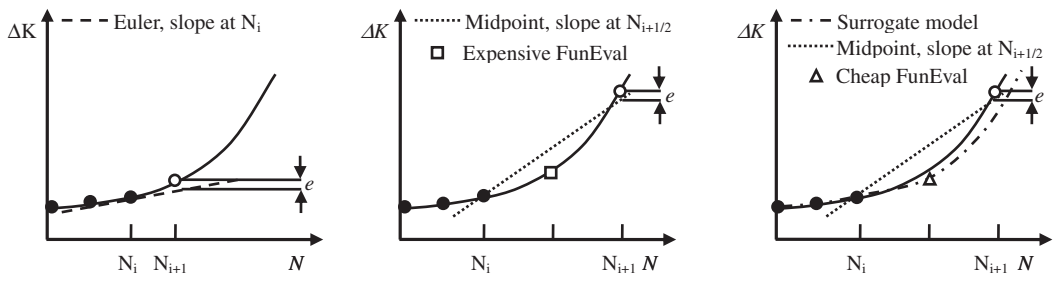

Fig. 2. Integration of fatigue crack growth model from N_i to N_{i+1} for a specified error e. For an unknown ΔK–a relationship, a simple integration method is the Euler method which uses the slope at N_i and extrapolates to N_{i+1}. To apply the midpoint integration method, which uses the slope at $N_{i+1/2}$ and extrapolates to N_{i+1}, an expensive function evaluation is required at $N_{i+1/2}$. Instead of an expensive function evaluation at $N_{i+1/2}$, it is proposed to fit a surrogate model to the ΔK–N history. The surrogate model is then used to extrapolate to $N_{i+1/2}$ enabling the use of high-order integration without additional expensive function evaluations.

α is an exponent which determines how quickly the step size changes, and ΔK_{i+1} and θ_{i+1} are evaluated based on $i+1$ for the current crack geometry using either a numerical (e.g. XFEM) or surrogate (e.g. kriging) model. The step size is scaled based on the accuracy of the predicted value. For the case where either $\Delta K_{i+1}^{SUR} = \Delta K_{i+1}^{NUM}$ or $\theta_{i+1}^{SUR} = \theta_{i+1}^{NUM}$, then $\Delta N_{i+1} = 2\Delta N_i$. The values of a_k and a_t in Eq. (3.1) were found to be 0.001, while α_t and α_k were defined to be 0.1 based on a parameter study.

A summary of this approach follows. A series of XFEM simulations were performed to evaluate ΔK^{NUM} as a function of the crack size a. In addition, the angle of crack growth given in terms of the global coordinate system θ^{NUM} was evaluated as a function of crack size. A brief summary of the XFEM is given in Appendix B. Once these easily evaluated functions were available, the crack growth was simulated such that:

1. For crack geometry i, fit surrogate for history of ΔK^{NUM} and θ^{NUM}, evaluate ΔK^{SUR} and θ^{SUR} at $i+1/2$ and $i+1$.
2. Calculate the crack growth increment Δa from $\Delta a = \Delta N_i C\left(\Delta K_{i+1/2}^{SUR}\right)^m$.
3. Calculate the crack growth increments in the x and y-directions from $\Delta x = \Delta a \cos\left(\theta_{i+1/2}^{SUR}\right)$ and $\Delta y = \Delta a \sin\left(\theta_{i+1/2}^{SUR}\right)$.
4. Update the crack tip location based on Δx and Δy followed by evaluating ΔK_{i+1}^{NUM} and θ_{i+1}^{NUM}.
5. Find the next step size based on the criteria in Eq. (3.1), repeat for next crack geometry.

4. Numerical experiments

4.1. Setup

First a center crack in an infinite plate under uniaxial tension is considered. This case is convenient as it has a closed form solution for the crack size and stress intensity factor as a function of applied stress, loading cycle, and material properties. This allows for an estimate of the amount of error that can be expected by the use of kriging to provide data points instead of performing a function evaluation. The effect on the choice of a fixed Δa or ΔN is considered for the theoretical model of a center crack in an infinite plate to show the validity of the approach. The presented variable step size algorithm is also used for each example problem. Results are presented for each case as the final approximate value normalized by the exact final value of crack size or cycle number. A value of one denotes perfect agreement with the exact solution.

The chosen geometry for all problems is a flat, square plate under uniaxial tension. The plate is considered to be infinite in problem A (Section 4.2) the plate width for problem B (Section 4.3) was 0.2 m, and the plate width for problem C (Section 4.4) was 2 m. For problems A and B, the applied uniaxial tension was 78.6 MPa. The applied stress for problem C was material dependent and is given in Table 7. The tested materials and the corresponding material properties are aluminum 2024 at stress ratios of 0.1 ($C = 1.60 \times 10^{-11}$, $m = 3.59$, $K_{IC} = 30$ MPa $\sqrt{m}$) and 0.5 ($C = 3.15 \times 10^{-11}$, $m = 3.59$, $K_{IC} = 30$ MPa $\sqrt{m}$) as well as austenitic ($C = 1.36 \times 10^{-10}$, $m = 2.25$, $K_{IC} = 50$ MPa $\sqrt{m}$) and martensitic ($C = 5.60 \times 10^{-12}$, $m = 3.25$, $K_{IC} = 50$ MPa $\sqrt{m}$) steel [38]. The results are presented for each case as a function of the ratio between the known solution and the prediction for either crack size or cycle number such that a value of one denotes the exact solution.

4.2. Center crack in an infinite plate under tension

First, a center crack in an infinite plate with initial crack length of 10 mm is considered. For the case of a center crack in an infinite plate under uniaxial tension, the Mode I stress intensity factor [7,8] is

$$K_I = \sigma\sqrt{\pi a} \tag{4.1}$$

where σ is the applied stress, and a is the half crack length. By substituting Eq. (4.1) into Eq. (2.1) for Paris model and rearranging terms, the number of cycles for a crack to grow can be calculated using the following integration:

$$N = \int_{a_i}^{a_N} \frac{da}{C(\sigma\sqrt{\pi a})^m} = \left[\frac{a_N^{\frac{2-m}{2}} - a_i^{\frac{2-m}{2}}}{C\left(\frac{2-m}{2}\right)(\sigma\sqrt{\pi})^m}\right] \tag{4.2}$$

where a_i is the initial crack size. Rearranging Eq. (4.2), the crack size a_N after N cycles can be calculated by

$$a_N = \left[NC\left(1 - \frac{m}{2}\right)(\sigma\sqrt{\pi})^m + a_i^{\frac{2-m}{2}}\right]^{\frac{2}{2-m}}. \tag{4.3}$$

This allows for the midpoint method to be applied as a_N and K_I can be directly evaluated and used in the integration of Paris model at any cycle number. For a geometry without known relationship between ΔK and a a finite element solution would need to be performed at N_i at which time an Euler approximation could be used to approximate $a_{i/2}$, allowing a second finite element simulation to be performed and the midpoint method to be applied.

An aluminum 2024 plate with a stress ratio of 0.5 is chosen to validate the use of kriging extrapolation for the integration of the fatigue crack growth model. The critical stress intensity factor is reached for a crack size of 50 mm given an initial crack size of 10 mm in about 22,300 cycles. For a fixed Δa, the results are given in Table 1. Recall that the common Δa used in the literature [3,4,6] is $a_i/10$. For that crack growth increment, the Euler approximation has over 5% error. Through the use of the midpoint approximation, the error is reduced to less than 1%. Larger crack growth increments for the Euler method lead to very large errors, which can be drastically reduced through the use of the midpoint approximation. Note also that the use of kriging to fit data and to interpolate estimates for the necessary function evaluations for the midpoint approximation results in no loss of accuracy. As interpolation is being used here, it would also be possible to apply other higher-order approximations such as the Runge–Kutta method [10] for the back-calculation of elapsed cycles for the case of a fixed Δa.

For a fixed ΔN, the results are given in Table 2. The first observation from Table 2 is that the accuracy of Euler approximations is much more sensitive to changes in fixed ΔN when compared to a fixed Δa. However, the midpoint approximations are largely insensitive to the chosen crack growth increment. As before, the kriging assisted midpoint approximation is very accurate and comparable to using the exact formula.

To assess the applicability of the variable step size algorithm to a range of fatigue problems four different materials were chosen along with initial crack sizes of either 1 or 10 mm and grown to failure at 50 mm. As with the fixed step size approach, three data points are found using the forward Euler approach with $\Delta N = 1$ before the variable step size algorithm begins. The results for the materials and crack sizes is given in Table 3.

Note that the number of function evaluations for the Euler method is the same as N_{fail}^{euler}. It can be noted from Table 3 that the number of function evaluations that the algorithm uses to model the crack growth to failure is generally independent of the number of cycles to failure. The general trend of the variable step size algorithm is that initially there are smaller steps, then the step size increases. When the crack approaches the critical crack size, the integration step size decreases ensuring an accurate solution. This behavior is shown in Section 4.4 in Fig. 4.

Table 1
Accuracy of kriging interpolation integration for fixed increment Δa for a center crack in an infinite plate of Al 2024 with $R = 0.5$. The data is presented as normalized values of the cycle at which the crack length is 50 mm. The kriging surrogate is used to calculate cycle number N for each discrete crack length a as a post-processing operation. Thus, all kriging evaluations are based on interpolation. The midpoint method was used here by evaluating Eq. (4.1) for any crack size a. This gives an error estimate for kriging interpolation.

Δa	Euler	FunEval	Midpoint	FunEval[a]	Kriging Interpolating Midpoint	FunEval
$a_i/160$	1.00	640	1.00	640	1.00	640
$a_i/80$	1.01	320	1.00	320	1.00	320
$a_i/40$	1.01	160	1.00	160	1.00	160
$a_i/20$	1.03	80	1.00	80	1.00	80
$a_i/10$	1.05	40	0.999	40	0.999	40
$a_i/5$	1.11	20	0.997	20	0.997	20
$a_i/2$	1.30	10	0.981	10	0.981	10
a_i	1.66	5	0.935	5	0.944	5

[a] For this problem since a closed for expression for a_N is available there are no additional function evaluations required for the midpoint method. For an arbitrary geometry where ΔK is evaluated using a numerical method, an additional function evaluation is needed between known data points, resulting double function evaluations compared to Euler and the kriging interpolating midpoint method.

Table 2
Accuracy of kriging extrapolation integration for fixed increment ΔN for a center crack in an infinite plate of Al 2024 with $R = 0.5$. The data is presented as normalized values of the crack length at cycle number 23,000. The kriging surrogate is used to extrapolate a stress intensity factor range allowing the midpoint method to be applied. While for a general crack direct application of the midpoint method is not possible, it is for this simple problem and provides an indication in the amount of error introduced by using kriging to replace expensive function evaluations.

ΔN	Euler	FunEval	Midpoint[a]	FunEval	Kriging extrapolating midpoint	FunEval
1	1.00	23,000	1.00	23,000	1.00	23,000
25	0.995	920	1.00	920	1.00	920
50	0.990	460	1.00	460	1.00	460
100	0.981	230	1.00	230	1.00	230
500	0.918	46	1.00	46	0.999	46
1000	0.856	23	0.999	23	0.995	23

[a] For a center crack in an infinite plate, the midpoint method can be used through Eq. (4.3). For an arbitrary geometry the midpoint method cannot be used. It is used here to assess the error introduced by the kriging extrapolation.

Table 3
Effect of material and initial crack size on estimated cycles to failure for the variable step size algorithm for a center crack in an infinite plate. Crack growth is simulated from initial crack length a_i until the crack a length of 50 mm. A comparison between the cycle where failure occurs based on the Euler N_{fail}^{euler} and kriging extrapolation N_{fail}^{KRG} methods is given in addition to the number of required function evaluations.

Material	a_i	N_{fail}^{euler}, FunEval^{euler}	N_{fail}^{KRG}	FunEval^{KRG}	N_{fail}^{KRG}/N_{fail}	FunEval^{KRG}/FunEval^{euler}
$R = 0.1$	1	364,676	369,169	49	1.01	1.34E-4
$R = 0.1$	10	43,237	43,437	38	1.00	8.79E-4
$R = 0.5$	1	185,232	188,126	48	1.02	2.59E-4
$R = 0.5$	10	21,962	22,053	38	1.00	1.70E-3
Austenitic	1	951,320	957,139	46	1.01	4.84E-5
Austenitic	10	428,539	429,546	46	1.00	1.07E-4
Martensitic	1	2193,024	2225,481	75	1.01	3.42E-5
Martensitic	10	435,647	438,664	47	1.01	1.08E-4

Table 4
Accuracy of kriging interpolation integration for fixed increment Δa for an edge crack in a finite plate of Al 2024 with $R = 0.5$. The data is presented as normalized values of the cycle at which the crack length is 50 mm. The kriging surrogate is used to calculate cycle number N for each discrete crack length a as a post-processing operation. Thus, all kriging evaluations are based on interpolation. The midpoint method was used here by evaluating Eq. (4.4) for any crack size a. This gives an error estimate for kriging interpolation.

Δa	Euler	FunEval	Midpoint	FunEval	Kriging interpolating midpoint	FunEval
$a_i/160$	1.00	640	0.996	640	0.996	640
$a_i/80$	1.00	320	0.996	320	0.996	320
$a_i/40$	1.01	160	0.996	160	0.996	160
$a_i/20$	1.03	80	0.995	80	0.996	80
$a_i/10$	1.07	40	0.995	40	0.994	40
$a_i/5$	1.14	20	0.991	20	0.991	20
$a_i/2$	1.39	8	0.969	8	0.973	8
a_i	1.88	4	0.905	4	0.944	4

4.3. Edge crack in a finite plate under tension

For the case of an edge crack in a finite plate under uniaxial tension, the Mode I stress intensity factor [7,8] is

$$K_I = \left[1.12 - 0.281\frac{a}{W} + 10.55\left(\frac{a}{W}\right)^2 - 21.72\left(\frac{a}{W}\right)^3 + 30.39\left(\frac{a}{W}\right)^4\right]\sigma\sqrt{\pi a} \tag{4.4}$$

where a is the crack length and W is the plate width.

Table 5
Accuracy of kriging extrapolation integration for fixed increment ΔN for an edge crack in a finite plate of Al 2024 with $R = 0.5$. The data is presented as normalized values of the crack length at cycle number 11,000. The kriging surrogate is used to extrapolate a stress intensity factor range allowing the midpoint method to be applied. The midpoint method may not be applied to this problem as no closed for solution for $a(N)$ is known to the authors for the stress intensity factor given by Eq. (4.4).

ΔN	Euler	FunEval	Midpoint[a]	FunEval[b]	Kriging extrapolating midpoint	FunEval
1	1.00	11,000	N/A	N/A	1.00	11,000
25	0.994	440	N/A	N/A	1.00	440
50	0.987	220	N/A	N/A	1.00	220
100	0.975	110	N/A	N/A	0.999	110
500	0.947	22	N/A	N/A	0.995	22
1000	0.877	11	N/A	N/A	0.978	11

[a] Due to the inability to exactly integrate Paris model with the stress intensity factor of Eq. (4.4), it is not possible to use the midpoint method for this problem. Nevertheless, when using a surrogate model to extrapolate, it is possible to apply the midpoint method to any problem based on the stress intensity factor range history.
[b] It would be possible to do a function evaluation for each N_i and then use a forward Euler step to find crack size $a_{i+1/2}$ at $N_{i+1/2}$. However, the number of function evaluations would double and additional error would be introduced by the forward Euler step used to find $a_{i+1/2}$.

Table 6
Effect of material and initial crack size on estimated cycles to failure for the variable step size algorithm for an edge crack in a finite plate. Crack growth is simulated from initial crack length a_i until the crack a length of 50 mm. A comparison between the cycle where failure occurs based on the Euler N_{fail}^{euler} and kriging extrapolation N_{fail}^{KRG} methods is given in addition to the number of required function evaluations.

Material	a_i	N_{fail}^{euler}, FunEval^{euler}	N_{fail}^{KRG}	FunEval^{KRG}	N_{fail}^{KRG}/N_{fai}	FunEval^{KRG}/FunEval^{euler}
$R = 0.1$	1	235,374	42	240,401	1.02	1.78E-4
$R = 0.1$	10	20,701	38	21,473	1.03	1.80E-3
$R = 0.5$	1	119,557	44	122,705	1.03	3.68E-4
$R = 0.5$	10	10,516	38	10,799	1.03	3.60E-3
Austenitic	1	594,634	49	601,308	1.01	8.24E-5
Austenitic	10	189,225	41	193,493	1.02	2.17E-4
Martensitic	1	1415,883	46	1459,668	1.03	3.25E-5
Martensitic	10	196,924	41	200,215	1.01	2.08E-4

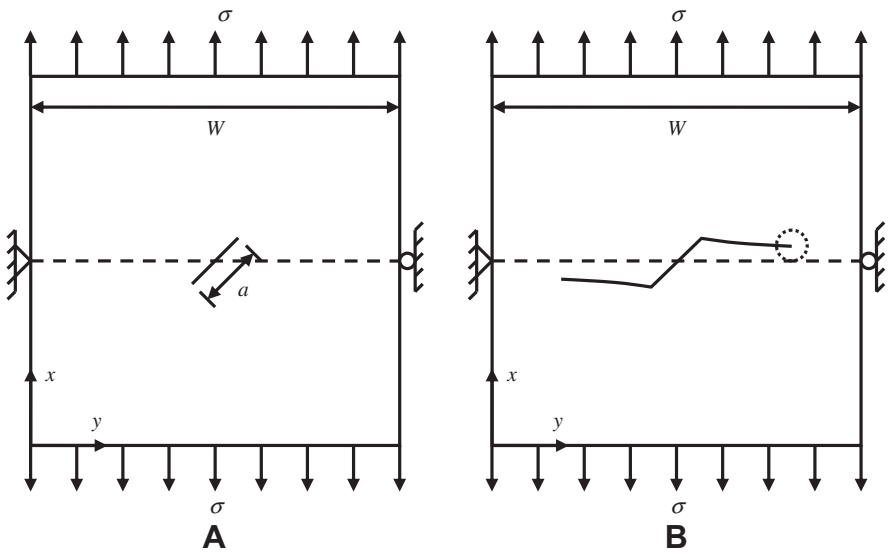

Fig. 3. Initial (A) and final (B) crack geometries for an inclined center crack in a square finite plate under uniaxial tension. XFEM was used to calculate the stress intensity factors and the crack growth direction was found from the stress intensity factors.

In this case, no analytical expression for a_N is available. The crack length after 10,700 cycles was found to be 30 mm using the forward Euler method (the step size was reduced until convergence in crack size at 10,700 cycles was achieved). For a fixed step size, aluminum 2024 with a stress ratio of 0.5 is chosen to validate the use of kriging extrapolation for the integration of the fatigue crack growth model with a constant step size. The critical stress intensity factor is reached for a crack size of 30 mm given an initial crack size of 10 mm in about 11,000 cycles, which is close to the reference value of 10,700 cycles. For a fixed Δa, the results are given in Table 4. Here for a fixed crack growth increment of $a_i/10$ the corresponding Euler approximation has an error of 7%, while the midpoint approximation yields less than 1% error.

For a fixed elapsed number of cycles in each function evaluation, the exact results for the midpoint method are not available as there is no explicit value for a_N. From Table 5 it is apparent that once again, the kriging assisted midpoint method allows for larger step sized compared to the forward Euler method. In this case, for a

Table 7
Comparison of Euler and variable step size predictions for the coordinates (X_{final}, Y_{final}) of the right crack tip marked with a dotted circle in Fig. 3 and cycle number N_{fail} corresponding to a final crack size of 0.6 m from an initial crack size of 0.187 m for four different materials. A comparison between the cycle where failure occurs based on the Euler N_{fail}^{euler} and kriging extrapolation N_{fail}^{KRG} methods is given in addition to the number of required function evaluations. Different stress levels were applied to different materials to reduce the cost associated with the number of XFEM simulations needed for the Euler method for austenitic and martensitic steel.

Material applied stress (Mpa)	Material (MPa)	Al 2024, $R = 0.1$ 50	Al 2024, $R = 0.5$ 50	Austenitic 125	Martensitic 75
X_{fail}, m	Euler	1.5431	1.5432	1.5431	1.5431
	Variable	1.5432	1.5433	1.5450	1.5431
Y_{fail}, m	Euler	1.0902	1.0902	1.0902	1.0902
	Variable	1.0902	1.0902	1.0900	1.0902
N_{fail}	Euler	29,519	14,996	68,331	80,597
	Variable	29,574	15,025	68,622	80,707
	FunEval^{KRG}	356	157	52	245

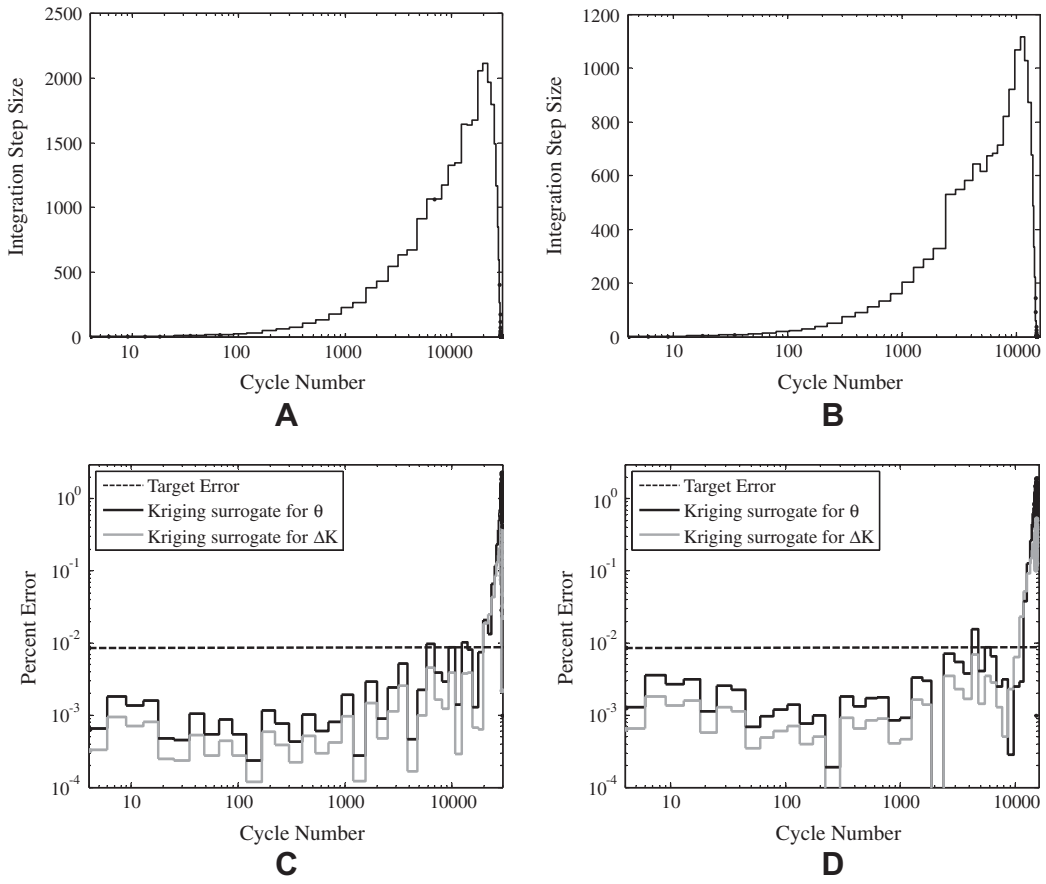

Fig. 4. Integration step size (A) and percent error (C) for each cycle for aluminum 2024, $R = 0.1$ as well as the step size (B) and percent error (D) for aluminum 2024, $R = 0.5$. The integration step size is based on the proposed variable step size algorithm. The percent error is given as the error in the kriging surrogate at the extrapolated point used for midpoint integration. Note that once the surrogate model has an error exceeding the target value, the step size is decreased.

step size of 100, the errors for the Euler and kriging assisted midpoint methods are 3.5% and 0.2%. The increased errors in the approximation compared to the case of a center crack in an infinite plate can most likely be explained by the increased nonlinearity caused by the edge and finite effects present in this geometry.

The variable step size algorithm is again tested with a range of fatigue problems. Four different materials were chosen along with initial crack sizes of either 1 or 10 mm and grown to failure at 50 mm. As with the fixed step size approach, three data points are found using the forward Euler approach with $\Delta N = 1$ before the variable step size algorithm begins. The previously determined values for a_k and a_t were found to be 0.0001, while α_t and α_k were defined to be 0.1 based on a parameter study. The results for the materials and crack sizes are given in Table 6. Note that there is an increased error for this case can be attributed to the a/W relationship present in Eq. (4.4).

4.4. Inclined center crack in a finite plate under uniaxial tension

The first test problem which also considers the effect of crack growth direction is that of an inclined center crack in a finite plate subjected to uniaxial tension in the y-direction as shown in Fig. 3. The plate was chosen to be a 2 m × 2 m plate with an initial half crack size of 0.187 m. The crack was grown by XFEM simulations

on a structured mesh of element size $h = 0.05$ m to a final half crack size of 0.6 m. The values of the constants in the variable step size algorithm were retained from the previous sections.

For the variable step size algorithm, different applied stresses were considered in order to make the Euler approximation feasible. The comparison of the number of cycles to failure and the final crack position for the Euler with constant $\Delta N = 1$ to the variable step size algorithm for the functions for ΔK and θ is presented in Table 7. Note that the cycle number corresponding to failure in each case is in excellent agreement with the XFEM solution, but with substantially less function evaluations are needed for the solution. The step size trends and the errors as a function of cycle number for both stress ratios for aluminum 2024 are given in Fig. 4.

5. Conclusions

The ordinary differential equation which governs fatigue crack growth is not easily solved because there is no analytical solution for complex geometries. In a general sense, the stress intensity factor can only be calculated at the current crack size using the extended finite element method. With that, it is common to take a forward Euler approach to the direct calculation of both the magnitude and direction of crack growth. To achieve sufficient accuracy, the forward Euler approach limits the step size and increases the number of function evaluations.

In this paper, kriging was used to fit the available history of the stress intensity factor and crack growth direction. The surrogate allows extrapolation ahead of the current data point, enabling the use of the midpoint approximation method for both stress intensity factor and crack growth direction. Additionally, an algorithm that adjusts the step size for a given allowable error was presented. The proposed approaches were demonstrated on a center crack in an infinite plate under uniaxial tension, an edge crack in a finite, and an inclined center crack in a square finite plate under uniaxial tension. It was found that:

- The use of surrogate modeling enables high order integration of crack growth, and
- the algorithm for adjusting the step size produces comparable accuracy with a significantly reduced number of function evaluations.

Results can be augmented with other problems to provide a more solid estimate of the savings associated with the procedure. In particular, the optimal choice of allowable prediction error and step size change exponent need to be studied. Future research also includes the use of uncertainty estimates available in certain surrogates (such as kriging) for further guidance on the integration step size.

Appendix A. Kriging surrogate

Surrogate modeling is a technique of approximating a function which is expensive to evaluate with one which is less expensive. Normally the approximation is done such that the error between the original function and approximate one is minimized at a given set of points. In this paper, the kriging [39–41] surrogate model is used to approximate a function of interest $y(\mathbf{x})$. As this function is expensive to evaluate, it may be approximated by a cheaper model $\hat{y}(\mathbf{x})$ based on assumptions on the nature of $y(\mathbf{x})$ and on the observed values of $y(\mathbf{x})$ at a set of p data points called experimental design. More explicitly,

$$y(\mathbf{x}) = \hat{y}(\mathbf{x}) + \varepsilon(\mathbf{x}), \tag{A.1}$$

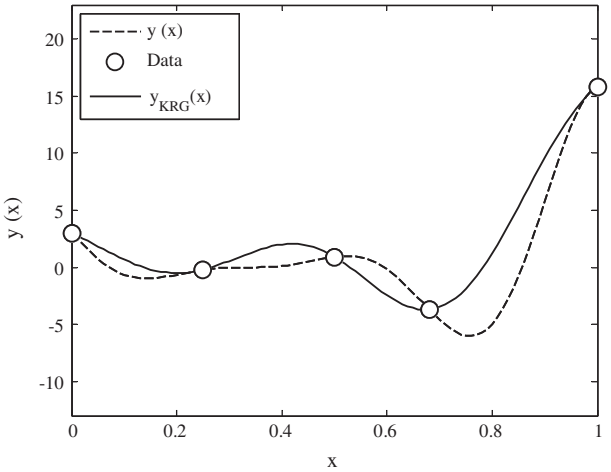

Fig. A1. Comparison of exact function and kriging model $y_{KRG}(\mathbf{x})$ for an arbitrary set of five points.

where $\mathbf{x} = [x_1, \ldots, x_d]^T$ is a real d-dimensional vector of input variables and $\varepsilon(\mathbf{x})$ represents both the error of approximation and random errors.

Kriging estimates the value of the unknown function $y(\mathbf{x})$ as a combination of basis functions $f_i(\mathbf{x})$ such as a polynomial basis and departures $z(\mathbf{x})$ as

$$\hat{y}(\mathbf{x}) = \sum_{i=1}^{m} \beta_i f_i(\mathbf{x}) + z(\mathbf{x}), \tag{A.2}$$

where $z(\mathbf{x})$ satisfies $z(\mathbf{x}_k) = y(\mathbf{x}_k) - \sum_{i=1}^{m} \beta_i f_i(\mathbf{x}_k)$ for all sample points $(\mathbf{x}_k)$ and is assumed to be a realization of a stochastic process $Z(\mathbf{x})$ with mean zero,

$$\mathrm{cov}(Z(\mathbf{x}_i), Z(\mathbf{x}_j)) = \sigma^2 R(\mathbf{x}_i, \mathbf{x}_j), \tag{A.3}$$

and process variance σ^2, and spatial covariance function given by

$$\sigma^2 = \frac{1}{p}(\mathbf{y} - \mathbf{X}\mathbf{b})^T \mathbf{R}^{-1} (\mathbf{y} - \mathbf{X}\mathbf{b}), \tag{A.4}$$

where $R(\mathbf{x}_i, \mathbf{x}_j)$ is the correlation between $Z(\mathbf{x}_i)$ and $Z(\mathbf{x}_j)$, $\mathbf{y}$ is the value of the actual responses at the sampled points, $\mathbf{X}$ is the Gramian design matrix constructed using the basis functions at the sample points, $\mathbf{R}$ is the matrix of correlations $R(\mathbf{x}_i, \mathbf{x}_j)$ among sample points, and $\mathbf{b}$ is an approximation of the vector of coefficients β_i of Eq. (A.2). Fig. A1 shows the prediction and the error estimates of kriging. It can be noticed that since the kriging model is an interpolator, the error vanishes at data points. The MATLAB SURROGATES Toolbox [42] was used in all numerical experiments.

Appendix B. Extended finite element method

Modeling crack growth in a traditional finite element framework is a challenging engineering task. Originally the finite element framework was modified to accommodate the discontinuities that are caused by phenomena such as cracks, inclusions and voids. The finite element framework is not well suited for modeling crack growth because the domain of interest is defined by the mesh. At each increment of crack growth, at least the domain surrounding the crack tip must be remeshed such that the updated crack geometry is accurately represented.

The extended finite element method [3,4,6] (XFEM) allows discontinuities to be represented independently of the finite element mesh. Arbitrarily oriented discontinuities can be modeled independent of the finite element mesh by enriching all elements cut by a discontinuity using enrichment functions satisfying the

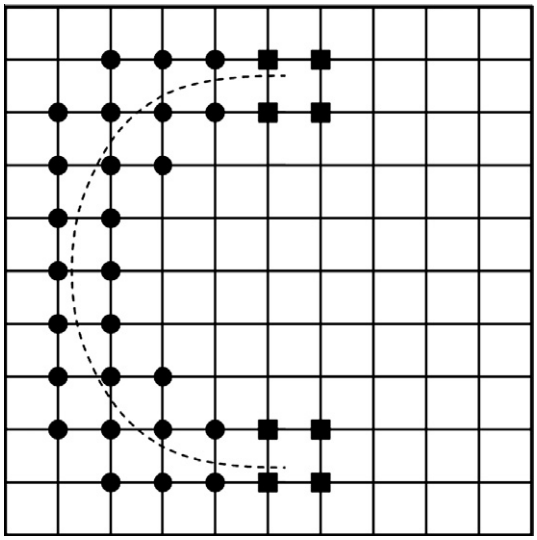

Fig. B1. The location of the enriched nodes corresponding to the crack enrichment functions where the Heaviside enriched nodes are filled circles and crack tip enriched nodes are filled squares for a crack represented by a dashed line.

discontinuous behavior and additional nodal degrees of freedom. For the case of a domain containing a crack [3] the approximation takes the form:

$$\mathbf{u}^h(x) = \sum_{I\in\Omega} N_I(x)\left[\mathbf{u}_I + \sum_{I\in\Omega_H} H(x)\mathbf{a}_I + \sum_{I\in\Omega_T}\sum_{\alpha=1}^{4}\Phi_\alpha(x)\mathbf{b}_I^\alpha\right] \tag{B.1}$$

where $N_I(x)$ are the traditional finite element shape function, $H(x)$ is the Heaviside enrichment function, $\Phi_\alpha(x)$ are the crack tip enrichment functions, and $\mathbf{u}_I$, $\mathbf{a}_I$, and $\mathbf{b}_I$ are the classical and enriched degrees of freedom. When a node would be enriched by the Heaviside and crack tip enrichment functions, only the crack tip functions are used as is shown in Fig. B1.

To decrease the computational time for the repeated solutions, a reanalysis algorithm [5] is used which takes advantage of the large constant portion of the global stiffness matrix. The mixed-mode stress intensity factors for the given cracked geometry were calculated using the domain form of the interaction integrals [43,44]. The direction of crack growth was calculated using the maximum circumferential stress criterion given by Eq. (2.3). The effective stress intensity factor was found from Eq. (2.2) and was used in Paris Law to calculate the magnitude of crack growth for a given crack geometry. MATLAB XFEM code [45] was used in the numerical experiment of an inclined center crack in a finite plate.

References

[1] Beden S, Abdullah S, Ariffin A. Review of fatigue crack propagation models in metallic components. Eur J Sci Res 2009;28:364–97.
[2] Maligno AR, Rajaratnam S, Leen SB, Williams EJ. A three-dimensional (3D) numerical study of fatigue crack growth using remeshing techniques. Eng Fract Mech 2010;77:94–111.
[3] Moes N, Dolbow JE, Belytschko T. A finite element method for crack growth without remeshing. Int J Num Meth Eng 1999;46:131–50.
[4] Sukumar N, Prévost JH. Modeling quasi-static crack growth with the extended finite element method. Part I: Computer implementation. Int J Solids Struct 2003;40:7513–37.
[5] Pais M, Kim NH, Davis T. Reanalysis of the extended finite element method for crack initiation and propagation. In: 51st AIAA/ASME/ASCE/AHS/ASC structures, structural dynamics, and materials conference, Orlando, Florida, 2010.
[6] Shi J, Chopp DL, Lua J, Sukumar N, Belytschko T. Abaqus implementation of extended finite element method using a level set representation for three-dimensional fatigue crack growth and life prediction. Eng Fract Mech 2010;77:2840–63.
[7] Murakami Y. Stress intensity factors handbook. New York: Pergamon Press; 1987.
[8] Tada H, Paris P, Irwin G. The stress analysis of cracks handbook. New York: ASME Press; 1987.
[9] Sankararaman S, Ling Y, Mahadevan S. Statistical inference of equivalent initial flaw size with complicated structural geometry and multi-axial variable amplitude loading. Int J Fatigue 2010;32:1689–700.
[10] Chapra S, Canale R. Numerical methods for engineering. New York: McGraw-Hill; 2002.
[11] Edke MS, Chang KH. Shape design sensitivity analysis (DSA) for structural fracture using extended FEM (XFEM). Int J Pure Appl Math 2008;49:365–72.
[12] Forrester AIJ, Keane AJ. Recent advances in surrogate-based optimization. Prog Aerosp Sci 2009;45:50–79.
[13] Queipo N, Haftka R, Shyy W, Goel T, Vaidyanathan R, Tucker P. Surrogate-based analysis and optimization. Prog Aerosp Sci 2005;41:1–28.
[14] Simpson TW, Toropov V, Balabanov V, Viana FAC. Design and analysis of computer experiments in multidisciplinary design optimization: a review of how far we have come – or not. In: 12th AIAA/ISSMO multidisciplinary analysis and optimization conference, Victoria, Canada, 2008.
[15] Wang G, Shan S. Review of metamodeling techniques in support of engineering design optimization. J Mech Des 2007;129:370–80.
[16] Paris P, Gomez M, Anderson W. A rational analytic theory of fatigue. Trend Eng 1961;13:9–14.
[17] Dabayeh AA, Topper TH. Changes in crack-opening stress after underload and overloads in aluminum alloy. Int J Fatigue 1995;17:261–9.
[18] Ibrahim FK, Thompson JC, Topper TH. A study of effect of mechanical variables of fatigue crack closure and propagation. Int J Fatigue 1986;8:135–42.
[19] Huang XP, Moan T. Improved modeling of the effect of *R*-ratio on crack growth rate. Int J Fatigue 2007;29:591–602.
[20] Kujawski D. A fatigue crack driving force parameter with load effects. Int J Fatigue 2001;23:S239–46.
[21] Xiaoping H, Moan T, Weicheng C. An engineering model of fatigue crack growth under variable amplitude loading. Int J Fatigue 2008;30:2–10.
[22] Tanaka K, Nakai Y, Yamashita M. Fatigue crack growth threshold for small cracks. Int J Fatigue 1981;17:519–33.
[23] Liu Y, Mahadevan S. Threshold stress intensity factor and crack growth rate prediction under mixed-mode loading. Eng Fract Mech 2007;74:332–45.
[24] Ray A, Patankar R. Fatigue crack growth under variable-amplitude loading: Part I – Model formulation in state-space setting. Appl Math Mod 2001;25:979–94.
[25] Ray A, Patankar R. Fatigue crack growth under variable-amplitude loading: Part II – Code development and model validation. Appl Math Mod 2001;25:995–1013.
[26] Lu Z, Liu Y. Small time scale fatigue crack growth analysis. Int J Fatigue 2010;32:1306–21.
[27] Rhee H, Salama M. Mixed-mode stress intensity factors solutions for a warped surface flaw by three-dimensional finite element analysis. Eng Fract Mech 1987;28:203–9.
[28] Tanaka K. Fatigue crack propagation from a crack inclined to the cyclic tension axis. Eng Fract Mech 1974;6:493–507.
[29] Yan X, Zhang Z. Mixed mode criteria for the materials with different yield strengths in tension and compression. Eng Fract Mech 1992;85:109–16.
[30] Bilby BA, Cardew GE. The crack with a kinked tip. Int J Fract 1975;11:708–12.
[31] Erdogan F, Sih GC. On the crack extension in plates under plane loading and transverse shear. J Basic Eng 1963;85:519–25.
[32] Nuismer RJ. An energy release rate criterion for mixed mode fracture. Int J Fatigue 1975;11:708–12.
[33] Richard HA, Fulland M, Sander M. Theoretical crack path prediction. Fatigue Fract Eng Mater Struct 2005;28:3–12.
[34] Sih GC. Strain-energy-density factor applied to mixed mode crack problem. Int J Fract 1974;10:305–21.
[35] Myers R. Classical and modern regression with applications. Pacific Grove: Duxbury Thomson Learning; 2000.
[36] Cheng B, Titterington D. Neural networks: a review from a statistical perspective. Stat Sci 1994;9:2–54.
[37] Smola A, Scholkopf B. A tutorial on support vector regression. Stat Comput 2004;14:199–222.
[38] Sun CT. Mechanics of aircraft structures. Hoboken: John Wiley and Sons; 2006.
[39] Kleijnen J. Kriging metamodeling in simulation: a review. Eur J Oper Res 2009;182:707–16.
[40] Martin J, Simpson TW. Use of kriging models to approximate deterministic computer models. AIAA J 2005;43:853–63.
[41] Stein M. Interpolation of spatial data: some theory for kriging. New York: Springer; 1999.
[42] Viana FAC. SURROGATES Toolbox User's Guide, Version 2.1; 2010. <http://www.sites.google.com/site/fchegury/surrogatestoolbox>.
[43] Shih C, Asaro R. Elastic–plastic analysis of crack on bimaterial interface. Part I – Small scale yielding. J Appl Mech 1988;55:299–316.
[44] Yau J, Wang S, Corten H. A mixed-mode crack analysis of isotropic solids using conservation laws of elasticity. J Appl Mech 1980;47:335–41.
[45] Pais M. MATLAB Extended Finite Element (MXFEM) Code, Version 1.2; 2010. <http://www.matthewpais.com/2Dcodes>.